OPTICAL STUDIES OF THE INFLUENCE OF MICROSCOPIC STRUCTURE ON THE OPTOELECTRONIC PROPERTIES OF 6.1Å-LATTICE CONSTANT III-V SUPERLATTICES

Final Report - February 2000

Contract No. N00014-99-1-0379

Submitted to the Office of Naval Research

by

Department of Physics & Astronomy, The University of Iowa, Iowa City, IA 52242

INVESTIGATORS

Thomas C. Hasenberg (PI), Associate Professor
(319) 335-1119 / thomas-Hasenberg@uiowa.edu

Michael E. Flatté (Co-PI), Assistant Professor
(319) 335-0144 / michael-flatte@uiowa.edu

Thomas F. Boggess (Co-PI), Professor
(319) 335-3520 / thomas-boggess@uiowa.edu

1. EXECUTIVE SUMMARY

The progress made in this 1-year grant is reported. The influence of the microscopic structure (particularly at material interfaces) on the optoelectronic properties of 6.1Å-lattice constant III-V superlattices is presented. Included are discussions of four research areas: 1) Theoretical studies of binary antimonide superlattices, 2) MBE growth of these superlattices, 3) Structural characterization using high-resolution X-ray diffraction (HRXRD), and 4) continuous-wave and ultrafast optical measurements of these superlattices.

The theoretical effort included spin lifetime calculations for bulk GaAs and InAs as well as for GaAs/AlGaAs and InGaAs/InP quantum wells. A fourteen bulk-band basis was utilized to account for the constituent zincblende symmetry. The spin lifetimes agree with recent experiments within experimental and theoretical error.

For the experimental effort, we grew multiple quantum well samples with InAs (7ML)/GaSb (12ML) superlattice quantum wells and AlSb barrier regions. Samples were grown with two different MBE growth procedures. The growth of the first group of samples involved 5-second Sb-soaks at the material interfaces, whereas growth of the second group employed migration-enhanced epitaxy (MEE) at the interfaces. Use of MEE was an attempt to realize more abrupt interfaces and reduce the defect concentrations in them.

The structures were characterized using time-resolved photoluminescence and time-resolved differential transmission. Excellent Shockley-Read-Hall lifetimes in the 4-5ns range were measured. Furthermore, spin lifetime measurements were made on a sample grown using the Sb-soaks as well as on a previous InAs/GaInSb/InAs/InGaAlAsSb 4-layer superlattice sample.

2. THEORETICAL STUDIES OF BINARY 6.1Å SUPERLATTICES

BACKGROUND

Potential applications of coherent spin states in quantum wells have led to new ultrafast optical studies of electron spin dynamics in these structures [1]. A crucial requirement of any spin technology is the ability to control the spin states and substantially extend the electron spin lifetime in these systems. Consequently, a full understanding of the spin relaxation mechanisms

is desirable. Electron spin relaxation in bulk zincblende semiconductors at room temperature is dominated by the D'yakonov-Perel' mechanism (DP), which is a direct result of the spin splitting of the conduction band due to the bulk inversion asymmetry (BIA) [2] of zincblende materials. D'yakonov and Kachorovskii have extended the above theory and have shown that the electron spin relaxation in zincblende type quantum well structures at room temperature is also mainly governed by the DP mechanism [3].

Recently, Terauchi {*et al*}. have experimentally investigated the electron spin lifetime in 75Å *n*-doped GaAs/ $Al_{0.4}Ga_{0.6}As$ quantum wells at room temperature [4]. The measured spin lifetimes are one order of magnitude longer than those predicted based on D'yakonov-Kachorovskii's (DK) theory [4]. A disparity of this degree calls for further improvement of the DK theory in order to satisfactorily explain the electron spin relaxation mechanism in GaAs/AlGaAs quantum wells.

Furthermore, recent experiments on InGaAs/InP quantum wells at room temperature again indicate the dominance of the DP mechanism. Spin splitting arising from interface effects has been proposed as the dominant contribution to the spin splitting of the quantum well minibands. The contribution of BIA in these systems, however, has not been evaluated.

TECHNIQUE

To accurately describe the DP spin relaxation mechanism in quantum wells we employ a heterostructure model based on a fourteen bulk band basis, which accounts for the zincblende symmetry of the heterostructure constituents. This should give results similar to those of the DP theory for bulk semiconductors such as GaAs and InAs. The DP calculations rely on a perturbative expansion of the electronic structure Hamiltonian near the zone center. This is reasonable in bulk materials at low dopings.

The DK theory for quantum wells, however, is also based on this perturbative expansion. Qualitatively it is similar to a single-band effective mass theory for quantum well states. It is well known that the single-band effective mass theory is limited in applications involving quantum well states, because the proper quantity (which plays the role of the effective mass) in quantum wells is energy dependent. In our fourteen-band basis the energy dependence of the

spin splitting is accounted for, at least within our restricted basis set. We note that a fourteen band model is the minimum size basis set which can properly account for zincblende symmetry in the bulk constituents of the quantum well.

RESULTS

Bulk GaAs: In Fig. 2-1 is shown a comparison of our calculations of the DP rate as a function of temperature for bulk GaAs *n*-doped at 10^{16} cm^{-3}. The experimental results come from J. M. Kikkawa and D. D. Awschalom.[1] Experimental values of the mobility were used to obtain the momentum scattering time as a function of temperature. An energy-independent momentum scattering time was assumed, and this seems a reasonable approximation except at the highest temperatures where phonon scattering dominates. At low temperature the calculated spin relaxation lifetime is too long; here the Elliot-Yafet (EY) mechanism is expected to dominate over the DP mechanism. Again a fourteen-band model for the electronic structure would be the best one to use to evaluate the EY spin relaxation rate.

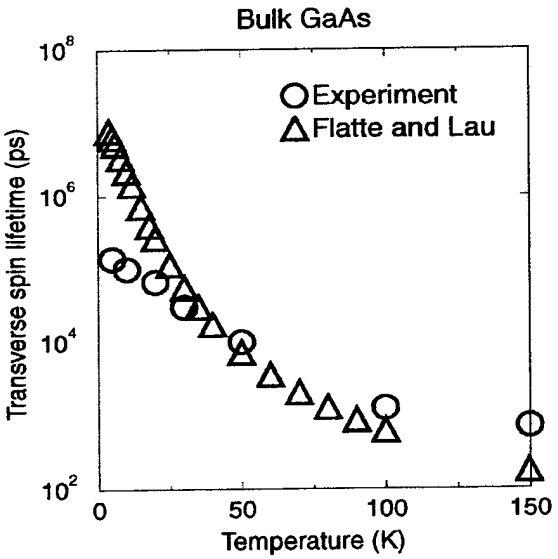

Fig. 2-1. Electron spin lifetimes in bulk GaAs as a function of temperature. Open circles represent the results of an experiment by Kikkawa and Awschalom[1], whereas open triangles represent our calculated values.

Bulk InAs: No experimental results for bulk InAs are available, but we have calculated the spin relaxation rate at 300K for n=1.7x 10^{16} cm^{-3} and a mobility of 3.3x 10^4 cm^2/Vs. This is a typical mobility for this carrier density. The resulting lifetime is 19.3ps. Note that if the doping and momentum scattering times are the same, the spin relaxation lifetime of InAs is about 2/3 that of GaAs. This difference originates as a result of the differences in the values of the effective mass, spin orbit splitting and band gap in InAs compared to GaAs.

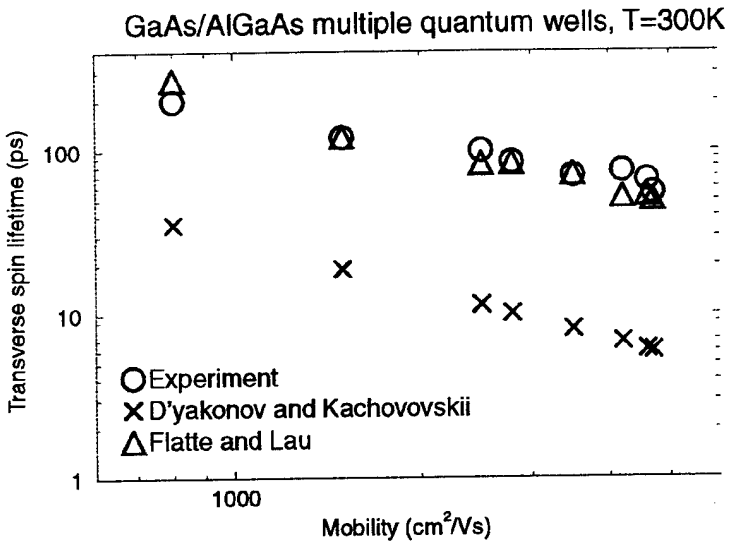

Fig. 2-2. Electron spin lifetimes at room temperature for different mobilities. The open circles represent the results of experiments by Terauchi et al. The triangles are our calculated values, whereas the crosses represent calculated values based on the D'yakonov and Kachorovskii theory.

GaAs/AlGaAs Quantum Wells: The calculated electron spin lifetimes for different mobilities are displayed in Fig. 2-2 along with the experimental results and the results of the calculated spin lifetimes based on the DK theory [4]. Our predicted spin lifetimes agree with the measured values within measurement error. In contrast, the calculated spin lifetimes based on the DK theory are an order of magnitude shorter than the experimental values. We note that the assumption of an energy-independent momentum scattering time is better suited to quantum well

applications than to bulk material, since interface roughness is likely to be the dominant cause of scattering in quantum wells.

InGaAs/InP Quantum Wells: Next we describe the spin splitting and spin lifetime in $In_{0.53}Ga_{0.47}As/InP$ quantum wells with 100Å barriers and wells ranging from 40Å to 100Å thick. The conduction subband spin splitting is dominated by the NIA mechanism for *thin* quantum wells, e.g., the 40Å well structure, whereas the spin splitting is governed by the BIA mechanism for *thick* quantum wells (e.g., the 70Å and 100Å well structures). We further note that the NIA mechanism is strongest for perfectly smooth interfaces, whereas BIA is insensitive to interface structure. We find that BIA provides a satisfactory explanation for the spin lifetime measured in an $In_{0.53}Ga_{0.47}As/InP$ quantum well with a 97Å barrier and a 70Å well at room temperature [6]. The theoretical value is 4.4 ps, which is within 20% of the experimental value of 5.2 ps.

3. MBE GROWTH

The materials effort involves superlattices composed of all-binary III-V compounds grown on GaSb substrates by MBE. The primary binary compounds investigated include InAs, GaSb and AlSb. The initial calibration samples grown contained InAs/GaSb superlattices (SL's) The InAs layers were 7 monolayers (ML's) thick and the GaSb layers were 12ML's thick. A series of samples were grown and subsequently examined with X-ray diffraction to determine and fine tune the individual layer thicknesses to the desired values. The details of this procedure are given in section 4. Next, multiple quantum well (MQW) samples with 8.5-period (*i.e.* starts and ends with InAs) InAs/GaSb superlattice (SL) quantum wells and with AlSb barrier layers were grown. A schematic diagram of the MQW structure is depicted in Fig. 3-1. The thicknesses of the InAs and GaSb layers in the SL were again 7MLs and 12 MLs, respectively. These thicknesses yield samples with layers that are thick enough for STM examination as well as in the correct wavelength range for MWIR pump/probe measurements. The peak of the photoluminescence (PL) wavelength is near 4.0μm (section 5). The AlSb barrier thicknesses were chosen to strain balance the InAs/GaSb 8.5 period SL. This should result in high quality coherently strained samples free of misfit dislocations. The presence of misfit dislocations

would color the results of the interfaces, lead to short Shockley-Read-Hall lifetimes, as well as make the structures difficult to cleave for STM studies.

The samples were grown in an EPI model 930 MBE machine. Valved cracker effusion cells were used for both the arsenic and antimony sources. The MBE shutter sequence for the initial structures involved the somewhat conventional (5-secs) Sb_2 soaks between the InAs and GaSb layers. Furthermore, the arsenic valve was closed during the growth of the GaSb and AlSb layers to minimize arsenic cross incorporation. This growth sequence should result in fairly pure InSb-like interfaces for the InAs on GaSb interfaces and mixed $InAs_xSb_{1-x}$ interfaces for the GaSb on InAs cases. This is because there is a partial exchange reaction of antimony for arsenic during the Sb-soaks after the InAs layers.

The net strain in the InAs/GaSb SL is largely dependent on the mole fraction (x) of arsenic in the mixed $InAs_xSb_{1-x}$ interfaces. This is the case because of the large lattice mismatch between InAs and GaSb (6.3%) in contrast to the relatively small mismatch between InAs and GaSb (0.62%). The first several samples were grown with 65ML thick AlSb barriers. This AlSb thickness would result in a strain balanced MQW structure if pure InAs MLs and pure InSb-like interface layers were realized just before the growth of the GaSb layers. However, this resulted in MQW structures with a substantial net strain. Clearly, mixed $InAs_xSb_{1-x}$ layers were present at the GaSb on InAs interfaces. Careful modeling of the results (see section 4) yielded an x-value of 0.8 (or 80% As in the $InAs_xSb_{1-x}$-like interfaces).

In order to further reduce the net strain, a series of InAs/GaSb SL samples was grown with 55ML AlSb barriers. As detailed in the next section, this resulted in a substantial reduction in the net strain to a value of 0.04%. This low value is lower than that of AlAs grown on GaAs and the material should be free of misfit dislocations caused by lattice mismatch.

Next we grew several samples using migration-enhance epitaxy at the material interfaces (i.e. GaSb/InAs interface). In this way we could "force" the interfaces to be one of two types (e.g. GaAs-like or InSb-like for the GaSb/InAs interface). The first samples utilized InSb-like interfaces at the both the GaSb/InAs interfaces and at the AlSb/InAs interfaces.

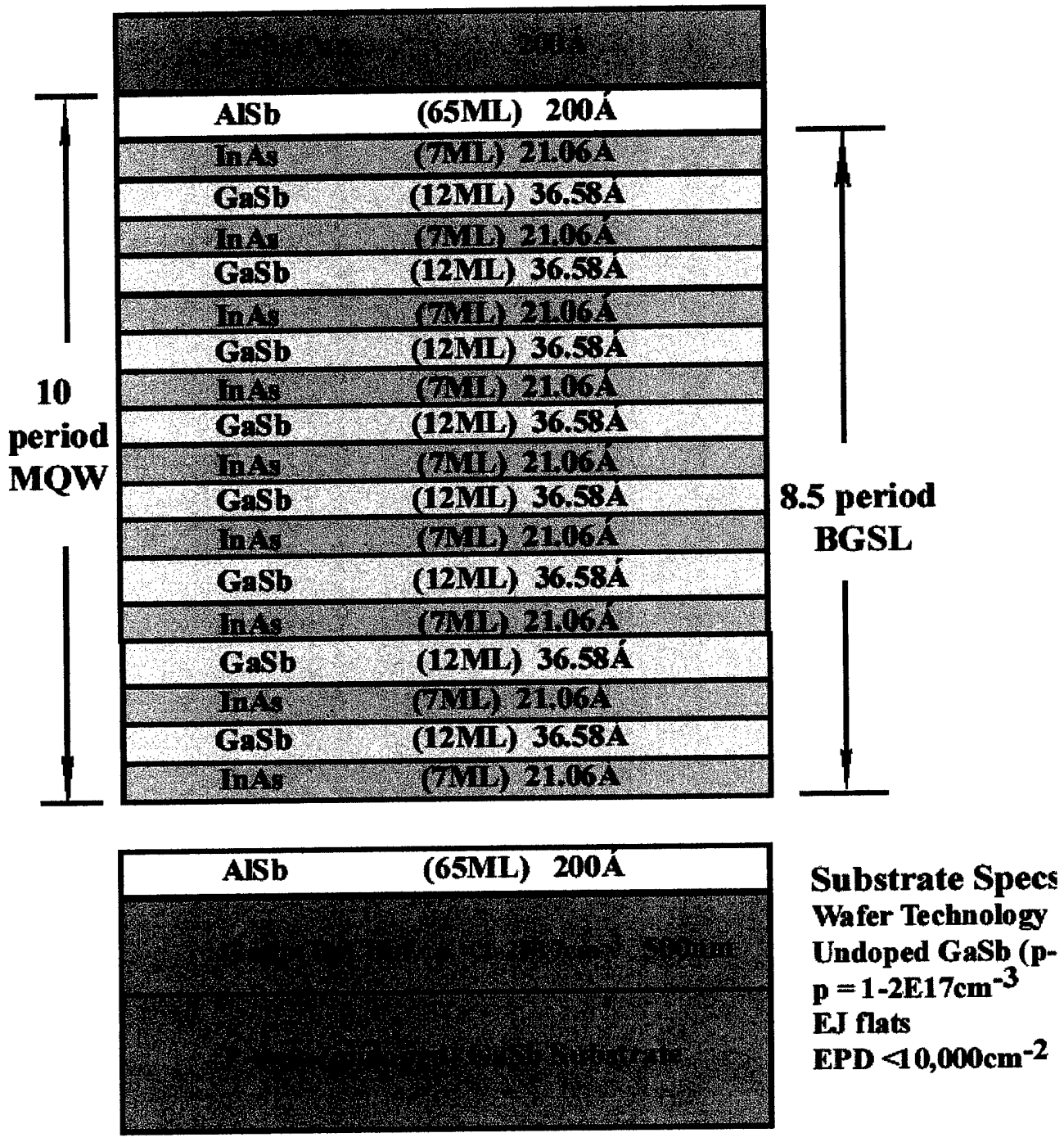

Fig. 3-1. Schematic diagram of a 10 period MQW structure with 8.5 period InAs/GaSb SL quantum wells and AlSb barriers.

4. CHARACTERIZATION BY X-RAY DIFFRACTION

High resolution X-ray diffraction (HRXRD) has been utilized to measure various parameters of the MBE grown superlattices using a BEDE model D1 diffractometer. The measurements include symmetric 004 reflections to determine the period of the superlattices. The initial InAs/GaSb SLs as well as the multiple quantum well (MQW) samples with InAs/GaSb SL wells and AlSb barriers were examined with the HRXRD system. The target structure was modeled with the dynamical X-ray model, and the input parameters were adjusted until a good fit was obtained between theory and experiment. Fig 4-1 shows the both the measured and the calculated X-ray diffraction spectra from an InAs(7ML)/GaSb(12ML) SL grown on GaSb. The excellent agreement between the experimentally measured X-ray spectrum and the one predicted with the dynamical X-ray simulation is indicative of abrupt interfaces and excellent precision and accuracy in the layer thicknesses. The only adjustable parameter (besides the InAs and GaSb layer thicknesses) in the dynamical model is the composition of the InAs/GaSb interface layers (i.e. $InAs_xSb_{1-x}$ instead of the desired InSb-like interface). By optimizing the fit between the experimental and modeled diffraction curves, we are able to determine the InAs and GaSb layer thicknesses as well as the composition of the InAsSb-like interface layers. Careful modeling of the results yielded an x-value of 0.2 (or 20% As in the $InAs_xSb_{1-x}$-like interfaces). The calibration procedure was repeated until samples with precise layer thicknesses were obtained (i.e. 7.0ML of InAs and 12.0ML of GaSb).

Next, these growth conditions were utilized to grow the aforementioned MQW samples with the InAs/GaSb SL's as the quantum wells. These MQW samples were analyzed in a similar way to the InAs/GaSb SL samples. As mentioned in section 3, the initial MQW samples had 65ML AlSb barriers. This barrier thickness would provide a stain-balanced MQW structure if pure InSb-like interfaces were obtained. However, with the mixed $InAs_{0.20}Sb_{0.80}$-like interface layers, we concluded that 55ML thick AlSb barrier layers were necessary to strain balance the InAs/GaSb SLs. An appropriate SL was grown (IA621) with the same 5-second Sb-soaks at the interfaces. The excellent effective lattice match of the MQW is evident from the position of the 0^{th} order peak, which corresponds to a strain of .04%. The intensity and sharpness of the superlattice satellite peaks are indicative of abrupt interfaces (Fig 4-2).

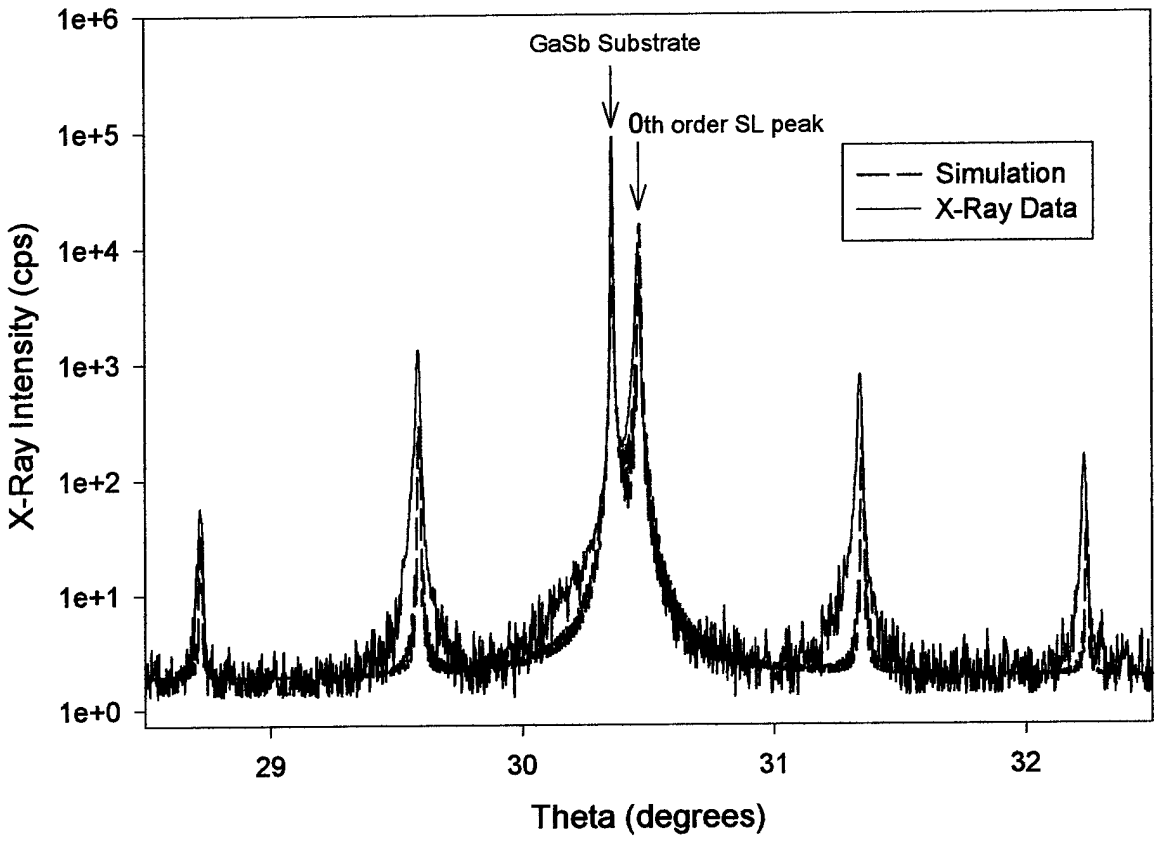

Figure 4-1. High-resolution X-ray diffraction for an InAs(7ML)/GaSb(12ML) superlattice (SL).

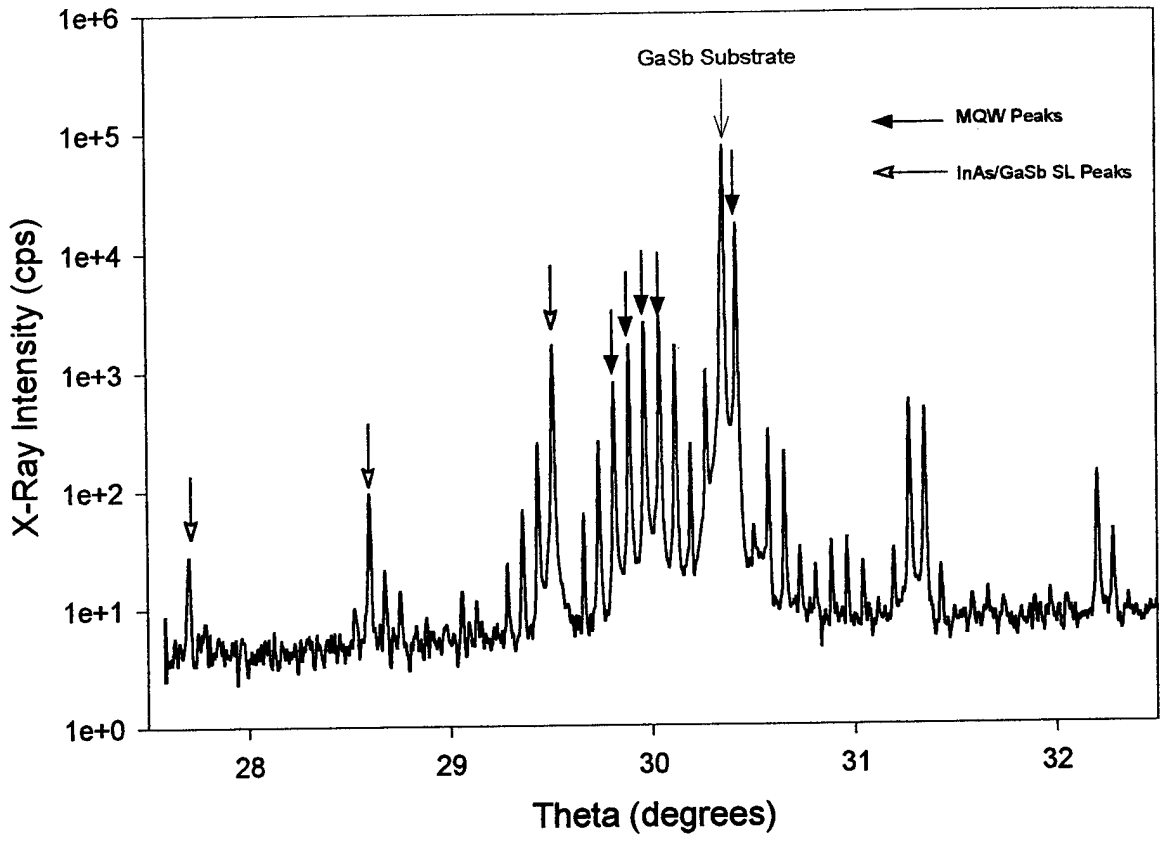

Figure 4-2. High-resolution X-ray diffraction for the MQW sample IA621. It contains InAs(7ML)/GaSb(12ML) SL quantum wells and 55 ML AlSb barriers.

5. Ultrafast Spectroscopy of InAs/GaSb Superlattices

We have measured the carrier dynamics in IA621 using a number of techniques. Initial measurements were directed at determining the quality of the sample by measuring the carrier recombination time. The results of time-resolved differential transmission measurements at 300K are shown in Fig. 5-1. These data were obtained using linearly-polarized excitation pulses at ~ 800nm and linearly-polarized probe pulses from the mid-IR OPO tuned to 3.63μm. These data reveal a SRH lifetime of approximately 5ns, indicating excellent material quality.

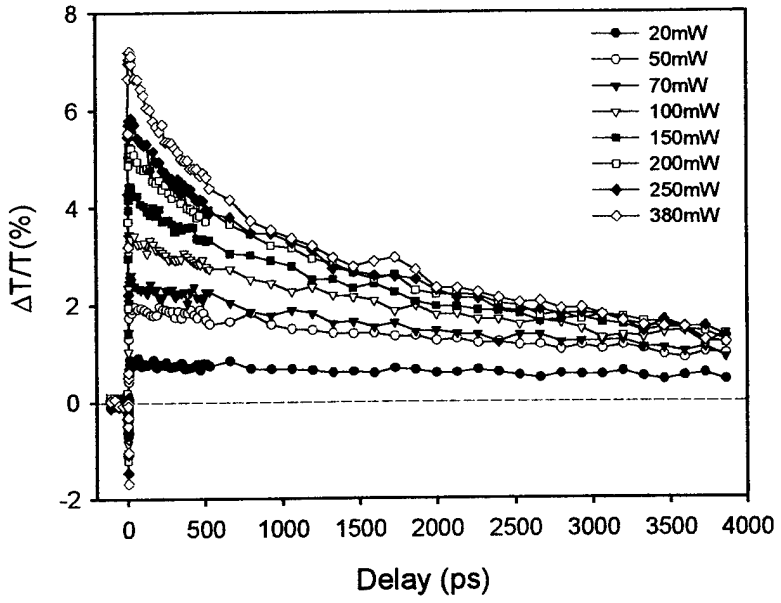

Figure. 5-1 Time-resolved differential transmission data for an MQW sample (IA621) with InAs/GaSb SL wells and AlSb barriers.

We have also performed polarization- and time-resolved differential transmission measurements in the InAs/GaSb superlattice labeled IA621. The measurement technique, which is illustrated in Fig. 5-2, relies on the excitation of the sample with circularly-polarized ultrashort pulses tuned near the band edge. In structures such as those of interest here, where the light- and heavy-hole levels are nondegenerate at zone center, the photo-excited carriers will be spin polarized (see Fig. 5-3) when excited with circularly polarized light. By probing this spin-polarized population with another ultrashort pulse, either of the same circular polarization (SCP) or opposite circular polarization (OCP) as that of the pump, we can interrogate either the decay of the photogenerated spin-polarized population, or the accumulation of a population of opposite spin orientation. By taking the difference in the two signals, we eliminate the effects of band filling associated with randomly polarized carriers, leaving a signal that exhibits only the spin decay. The difference data typically display an exponential decay with a time constant that is half the spin relaxation time.

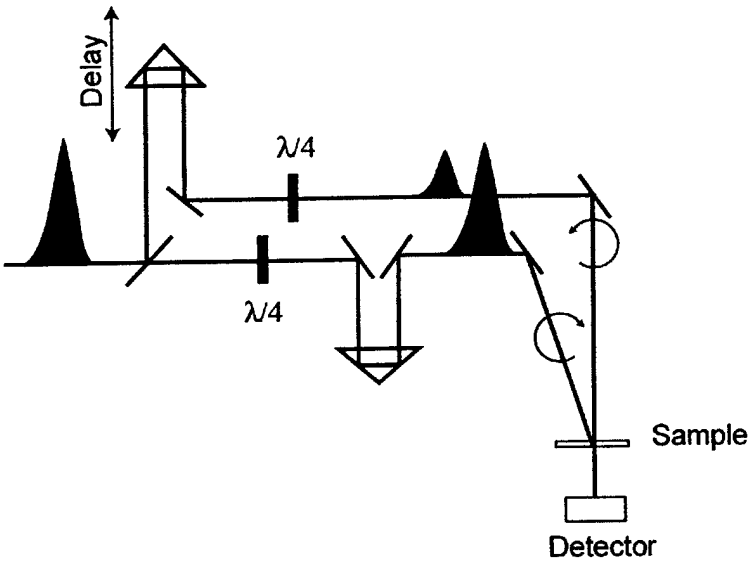

Figure 5-2. Schematic of pump-probe configuration used for spin relaxation measurements.

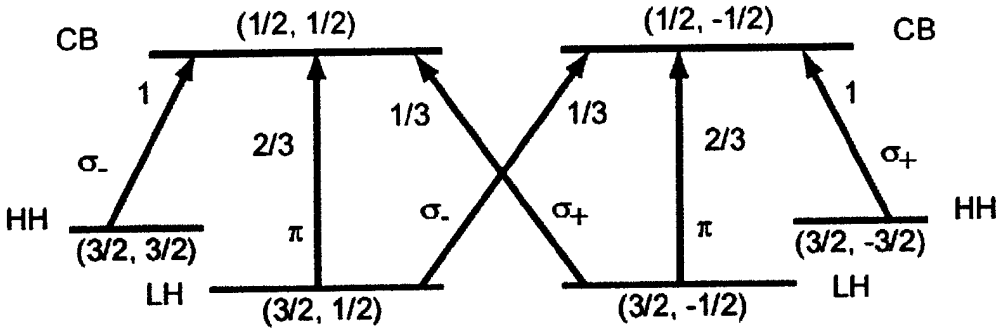

Figure 5-3. Selection rules and relative transition strengths for circular (σ_+ and σ_-) and linear (π) polarized excitation of a III-V quantum well or superlattice.

Data for IA621 are shown in Figure 5-4 for temperatures of 300 and 180 K. For these measurements, the excess excitation energy was kept constant and below the expected optical phonon energy. The data clearly display the anticipated features of a decay from an essentially 100% spin polarized initial population to a randomly oriented spin population for the SCP case and a build up of population in the spin state opposite that of the photogenerated carriers in the OCP case. In addition, for both temperatures, we observe an extremely rapid spin relaxation time. The relaxation time is quantitatively analyzed by fitting the data in Fig. 5-5, which shows the difference signal (SCP-OCP) for the two temperatures. This yields a spin relaxation time of 0.25 ps and 1.1 ps for the 300 and 180K data, respectively. The rapid and relatively strong

temperature dependence of the relaxation rate are consistent with relaxation through the D'yakonov-Perel mechanism.

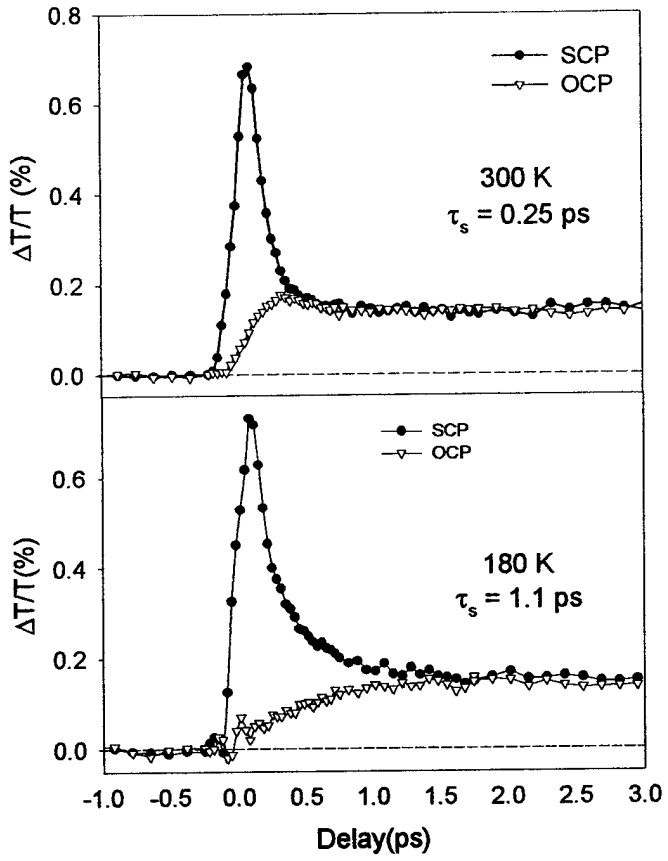

Figure 5-4. Time-resolved differential transmission measurements of the spin relaxation time in IA621 for temperatures of 300 and 180 K. In each case, the two data sets are obtained with either the probe configured with the same circular polarization as the pump (SCP) or opposite circular polarization (OCP).

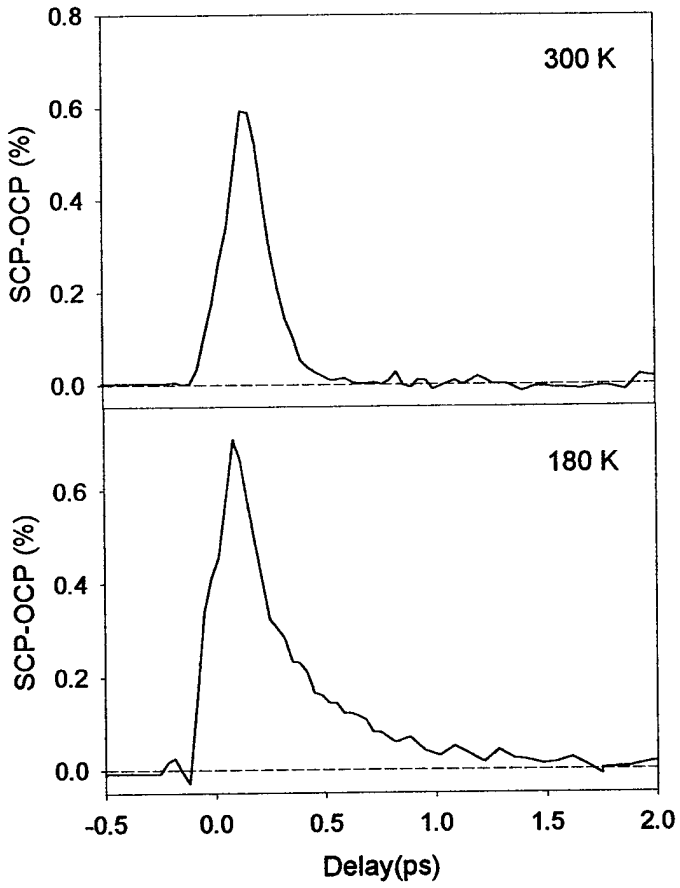

Figure 5-5. Difference signal (SCP-OCP) for the data shown in Fig. 5-4. The spin relaxation times are extracted from exponential fits to the decaying signals, taking into account the finite duration of the optical pulses.

SUMMARY

Clearly the 6.1Å material system is an interesting one with unique problems due to the often encountered non-common atom (NCA) interfaces (e.g. GaSb/InAs interface). The initial work has been done to grow very high quality samples with excellent precision and accuracy in the individual layer thicknesses. Sets of such samples have been grown with intentionally varying degrees of interface abruptness at these NCA interfaces. Characterization procedures have been initiated in an attempt to determine the chemical nature and relative importance of these defects at the NCA interfaces. Furthermore, initial spin lifetime measurements have been performed on several of these 6.1Å samples. It is likely that these measurements will yield new information

about the interfaces since interface roughness has been proposed as the dominant contribution to the spin splitting of the quantum well minibands. Finally, the heterostructure model based on a fourteen bulk band basis has been utilized to perform spin lifetime calculations for bulk GaAs and InAs as well as for GaAs/AlGaAs and InGaAs/InP quantum wells. Calculations for spin lifetimes of the 6.1Å materials should be underway in the near future. .

REFERENCES

[1] J. M. Kikkawa and D. D. Awschalom, Phys. Rev. Lett. **80**, 4313 (1998).

[2] M. I. D'yakonov and V. I. Perel', Sov. Phys. Solid State **13**, 3023 (1972).

[3] M. I. D'yakonov and V. Yu. Kachorovskii, Sov. Phys. Semicond. **20**, 110 (1986).

[4] R. Terauchi, Y. Ohno, T. Adachi, A. Sato, F. Matsukura, A. Tacheuchi, and H. Ohno, Jpn. J. Appl. Phys. **38**, Pt. 1, No. 4B, 2549 (1999).

[5] L. Vervoort, R. Ferreira, and L. P. Voisin, Sov. Phys. Solid State **14**, 227 (1999).

[6] A. Tacheuchi, O. Wada, and Y. Nishikawa, Appl. Phys. Lett. **70**, 1131 (1997).

REPORT DOCUMENTATION PAGE

Form Approved
OMB No. 0704-0188

1. AGENCY USE ONLY *(Leave blank)*	2. REPORT DATE 2/2000	3. REPORT TYPE AND DATES COVERED Final 1/99-1/00

4. TITLE AND SUBTITLE
Optical Studies of the Influence of Microscopic Structures on the Optoelectronic Properties Of 6.1Å-Lattice Constant III-V Superlattices

5. FUNDING NUMBERS
C- N00014-99-1-0379

6. AUTHORS
Thomas C. Hasenberg, Thomas F. Boggess and Michael E. Flatte

7. PERFORMING ORGANIZATION NAME(S) AND ADDRESS(ES)
University of Iowa
Iowa City IA 52242

8. PERFORMING ORGANIZATION REPORT NUMBER

8. SPONSORING/MONITORING AGENCY NAME(S) AND ADDRESS(ES)
Office of Naval Research
Ballston Centre Tower One
800 N Wuincy St
Arlington, VA 22217-5660

10. SPONSORING/MONITORING AGENCY REPORT NUMBER

11. SUPPLEMENTARY NOTES

12a. DISTRIBUTION/AVAILABILITY STATEMENT
Approved for Public Release; distribution is unlimited.

12b. DISTRIBUTION CODE

13. ABSTRACT *(Maximum 200 words)*

The influence of the microscopic structure (particularly at material interfaces) on the optoelectronic properties of 6.1Å-lattice constant III-V superlattices is presented. Included are discussions of four research areas: 1) Theoretical studies of binary antimonide superlattices, 2) MBE growth of these superlattices, 3) Structural characterization using X-ray diffraction, and 4) continuous-wave and ultrafast optical characterization.

The theoretical effort included spin lifetime calculations for bulk GaAs and InAs as well as for GaAs/AlGaAs and InGaAs/InP quantum wells. A fourteen bulk-band basis was utilized to account for the constituent zincblende symmetry. The spin lifetimes agree with recent experiments within experimental and theoretical error.

The experimental effort, multiple quantum well samples were grown with InAs (7ML)/GaSb (12ML) superlattice quantum wells and AlSb barrier regions. Two different MBE growth procedures were used at the material interfaces: 1). 5-second Sb-soaks and 2) migration-enhanced epitaxy (MEE). Use of MEE was an attempt to realize more abrupt interfaces and reduce the defect concentrations.

The structures were characterized using time-resolved photoluminescence and time-resolved differential transmission. Excellent Shockley-Read-Hall lifetimes in the 4-5ns range were measured. Furthermore, spin lifetime measurements were made on a sample grown using the Sb-soaks as well as on a previous InAs/GaInSb/InAs/InGaAlAsSb 4-layer superlattice sample.

14. SUBJECT TERMS 6.1Å materials; superlattices; interfaces; III-V semiconductors; GaSb; Spin Lifetimes; MBE growth; defects; Pump probe measurements

15. NUMBER OF PAGES
16

16. PRICE CODE

17. SECURITY CLASSIFICATION OF REPORT	18. SECURITY CLASSIFICATION OF THIS PAGE	19. SECURITY CLASSIFICATION OF ABSTRACT	20. LIMITATION OF ABSTRACT
Unclass	Unclass	Unclass	UL